García Martínez, A.; Monsalve-Serrano, J.; Villalta-Lara, D.; Zubel, M.; Pischinger, S. (01-1). Potential of 1-octanol and di-n-butyl ether (DNBE) to improve the performance and reduce the emissions of a direct injected compression ignition diesel engine. Energy Conversion and Management. 177:563-571. https://doi.org/10.1016/j.enconman.2018.10.009

Potential of 1-octanol and di-n-butyl ether (DNBE) to improve the performance and reduce the emissions of a direct injected compression ignition diesel engine

Antonio García[a,*], Javier Monsalve-Serrano[a], David Villalta[a], Marius Zubel[b], Stefan Pischinger[b]

a- CMT - Motores Térmicos, Universitat Politècnica de València, Camino de Vera s/n, 46022 Valencia, Spain
b- Institute for Combustion Engines, RWTH Aachen University, Aachen, Germany

Corresponding author (*):
Dr. Antonio García Martínez (angarma8@mot.upv.es)
Phone: +34 963876574
Fax: +34 963876574

Abstract

This experimental work evaluates the potential of 1-octanol, di-n-butyl ether and three intermediate blends as substitutes of the diesel fuel to be used in compression ignition engines. For this purpose, performance and engine-out emissions measurements have been done in a single-cylinder engine of 0.39 liter displacement and 15:1 compression ratio at four engine operating conditions representative of the new European driving cycle (NEDC) driving cycle. The tests have been done keeping constant the NOx emissions and combustion center for all the fuels at each operating point. To achieve this, the exhaust gas recirculation rate and the start of injection timing were modified simultaneously for each fuel tested, while the rest of the engine settings were kept constant. All the biomass-derived fuels have the same oxygen content but substantially different cetane number and volatility.

The results show that, for the same NOx levels, all the fuels allow a substantial reduction of the soot emissions versus diesel due to both the higher oxygen content in the fuel molecule and/or the extended mixing time achieved because of the lower fuel reactivity. In terms of efficiency, all the alternative fuels improve the fuel-to-work conversion efficiency. This benefit comes from decreasing the heat transfer in a greater way than the exhaust losses increase. Moreover, in general terms, all the fuels promote a reduction of the combustion losses to halve of those found with diesel.

Keywords

Fuel blends; biomass-derived fuels; diesel engine; emissions

1. Introduction

The internal combustion engines (ICE) play a fundamental role to cover primary services from the lifestyle of the current society, such as freight transportation and people mobility [1]. For this reason, the car ownership rate in the developed countries

has an historical growing trend over the years [2]. As a counterpart, the massive use of the ICEs has short- and long-term effects on the environment, such as the air quality worsening in the cities and the ozone layer degradation [3][4]. Moreover, the extended use of ICEs is aggravating the crude oil reserves depletion [5]. Hence, the engine research community is focused on developing more efficient internal combustion engines by optimizing the existing combustion systems and studying new combustion modes [6]-[8]. In parallel to developing the ICE components, the researchers are evaluating the use of new fuels to promote an environmentally friendlier ICE operation [9]. One example is the Cluster of Excellence "Tailor-Made Fuels from Biomass" (TMFB), which was established in 2007 at RWTH Aachen University [10]. The long-term goal of this research program is the establishment of a model based fuel design process for lignocellulose derived feedstocks which simultaneously considers both, fuel production and fuel-to-work conversion in engines [11]. To achieve this, several promising biofuel candidates for spark ignition (SI) and compression ignition (CI) engines were investigated during the past decade [12]-[16].

Two of the most promising biofuels to be used in the future CI engines are 1-Octanol and di-n-butyl ether (DNBE), which are isomers with the same formula ($C_8H_{18}O$). 1-octanol can be produced satisfactorily through a novel catalyst system starting from the platform molecules furfural and acetone [17]-[19] and DNBE can be obtained via etherification of n-butanol. In spite of having the same formula, their combustion-related properties are completely different due to the different position of the oxygen atom within the molecule [20]. While DNBE shows a very high reactivity, 1-octanol has lower reactivity than conventional diesel fuel. Furthermore, DNBE has a higher volatility and faster spray breakup due to the higher volatility and lower surface tension as well as dynamic viscosity [21].

Recent works have demonstrated that 1-octanol has several properties that benefit the combustion process in CI engines [22]. In this sense, it was found that the increased oxygen content provides an enhanced combustion with higher thermal efficiency than with diesel [23]. In terms of emissions, lower NOx and soot levels than with diesel fuel were reported in literature. The decrease in NOx emissions with 1-octanol was attributed to its lower boiling point, while the soot reduction was attributed to the higher oxygen content and ignition delay [23]. However, the CO and HC emission levels with 1-octanol were moderately increased due to the longer ignition delay period as compared to that of diesel fuel [24]. Finally, some recent studies performed using n-octanol/diesel blends showed considerable reductions in particulate matter (PM) thanks to the addition of n-octanol, leading to a better NOx/PM trade-off than diesel fuel, and with lower HC and CO emissions than with a single-fuel combustion of 1-octanol [25][26].

Fundamental aspects about DNBE fuel have been already investigated in literature, as per example its detailed kinetic reaction mechanisms [27], production process [28], spray formation [29], and unburnt hydrocarbon emissions characterization [30]. Experimental works in a single-cylinder engine have demonstrated that DBNE allow a good balance between efficiency, emissions and combustion noise [31]. The greatest advantage of DNBE compared to 1-octanol is obtained at low load, where the high reactivity of DNBE leads to higher thermal efficiency and lower HC and CO emissions [32].

From the literature review, it can be concluded that the use of 1-octanol can allow increasing the thermal efficiency of the engine with lower soot and higher HC and CO emissions than diesel fuel. When n-octanol is mixed with diesel fuel, the NOx/PM trade-off is still better than that found with diesel, and the HC and CO emissions levels are lower than those found with 1-octanol because of the higher reactivity of the mixture. On the other hand, it has been found that DNBE is a promising high-reactivity oxygenated fuel that can be a potential candidate to substitute the diesel fuel. Because of its high reactivity, DNBE fuel cannot offer extended ignition delays as those achieved with 1-octanol, which allow increasing the thermal efficiency. However, DNBE can be though to be mixed with 1-octanol to obtain the benefits found with n-octanol/diesel blends. In this sense, the potential benefits with DNBE are expected to be higher due to its properties compared to diesel fuel, as per example the higher oxygen content. Therefore, the objective of the present study is the characterization of the combustion process of 1-octanol/DNBE mixtures at different ratios. With this approach, the reactivity of the fuel blend can be adjusted and the physical properties can be tuned to be more similar to conventional diesel fuel. To assess the potential of such fuels in real conditions, the performance and engine-out emissions measurements have been done in a single-cylinder engine of 0.39 liter displacement and 15:1 compression ratio at four engine operating conditions representative of the new European driving cycle (NEDC) driving cycle.

2. Materials and methods

2.1. Engine characteristics and test cell description

The experimental tests were done in a single-cylinder 0.39 L displacement compression ignition (CI) engine. The engine has four valves driven by dual overhead camshafts. The piston has a ω-shaped re-entrant bowl with a volume of 21.6 cm^3 and the squish height is 0.78 mm. The geometric compression ratio of the engine is 15:1. The injector used is a piezo-electric type unit fed by a common rail system that enables a maximum injection pressure of 2200 bar. The maximum specific power output of the engine is 80 kW/l, with maximum in-cylinder pressures up to 190 bar. Table 1 summarizes the more relevant characteristics of the engine [33].

The scheme of the test cell in which the engine is operated is shown in Figure 1. The fuel consumption and the volumetric air flow are measured by means of a Coriolis-type fuel flow meter and an ultrasonic gas meter, respectively. Later, the air mass flow is calculated considering its temperature and water content. An external charging system is used to boost the engine with the desired pressure. Four charge air coolers connected in series are used to control the air temperature before entering to the cylinder. An electric position-controlled exhaust gas recirculation (EGR) valve is used for adjusting the EGR rate, which is calculated considering the CO_2 concentration at the intake and exhaust manifolds. The in-cylinder pressure is recorded via FEV's combustion analyzing system using a water cooled piezoelectric pressure transducer Kistler 6041A, and with an angular resolution of 0.1 crank angle degree (CAD). The rest of the pressures along the systems are recorded at angular increments of 0.5 CAD. The exhaust gas back-pressure is controlled with two valves located at the exhaust gas line, at the end of which the engine-out emissions are measured. The concentrations of HC, O_2, CO and CO_2 are measured using a Rosemount NGA 2000 system. NO_x emissions are measured by means of a chemiluminescence analyzer Eco Physics 700 EL ht. Finally,

the black carbon contained in the particulate matter is measured with an AVL 415S smoke meter. The sampling lines for the HC, CO, and NOx measurements are heated up to 180 °C to avoid condensation. The sample line of the Smoke Meter is heated to 75 °C.

Table 1. Single-cylinder engine specifications.

Displacement [cm³]	390
Stroke [mm]	88.3
Bore [mm]	75
Compression ratio [-]	15:1
Valves/cylinders number [-]	4
Max. cylinder pressure [bar]	190
Fuel injection [-]	Piezo Common rail
Max. injection pressure [bar]	2200
Max. boost pressure [bar abs.]	3.8

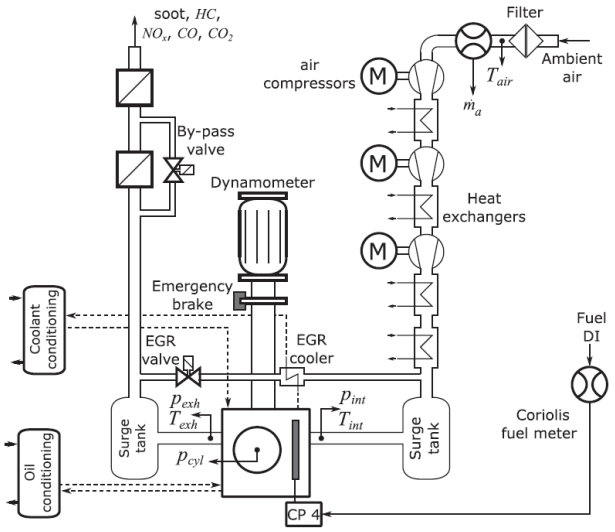

Figure 1. Test cell scheme. Adapted from [34].

2.2. Fuels characteristics

The more relevant chemical and physical characteristics of 1-octanol and DNBE fuels are listed in Table 2 [35]-[38]. Apart from the two base fuels, several intermediate blends are tested in the study. The physical properties of the blends were determined assuming linear blending rules and the cetane number (CN) was determined using the Advanced Fuel Ignition Delay Analyzer (AFIDA) [39]. Along the manuscript, the different fuel blends will be named considering the percentage content of the base fuels, e.g. O20D80 means a blend of 20% 1-octanol and 80% BNDE. The properties of the reference diesel fuel that will be used for comparison are also depicted in the table.

Table 2. Characteristics of the fuels used in this work.

	Diesel	1-octanol	O80D20	O50D50	O20D80	DNBE
Boiling temperature [°C]	180-350	195	141-195	141-195	141-195	141
Lower Heating value [MJ/kg]	42.9	37.6	37.68	37.8	37.92	38
Density [kg/m^3]	833	817	808	794	779	770
Cetane number [-]	56	37	45	58	81	~105
Oxygen content [% m/m]	0.14	12.3	12.3	12.3	12.3	12.3
Vapor Pressure [mbar]	<1	0.125	1.38	3.26	5.15	6.4
Surface Tension [mN/m]	20.5	27.5	26.4	24.9	23.3	22.2
Kinematic Viscosity @ 40 °C [mm^2/s]	3	7.3	5.97	3.97	1.97	0.64
Heat of Vaporization [kJ/kg]	358	562	519	454	389	346

2.3. In-cylinder pressure signal processing

The combustion analysis was done by means of an in-house developed software called CALMEC [40][41]. This single-zone combustion model allows calculating the burning rates, mass fraction burned, ignition delay and energy terms, among others, to characterize the combustion process. To do this, the different high and low frequency variables acquired during the engine experiments such as engine speed, inlet and exhaust temperatures from oil and coolant, air mass flow, EGR rate, fuel mass and some others, must be used as inputs for CALMEC.

Apart from those variables, CALMEC is fed with the instantaneous pressure traces of 50 consecutive engine cycles for each operating point, which enables the analysis of the cycle-to-cycle variation. The individual raw pressure data are smoothed using a Fourier series low-pass filter. Later, the smoothed cycles are averaged to obtain a representative cylinder pressure trace, which is used to perform the analysis of the combustion process. For this purpose, the first law of thermodynamics is applied between the intake valve closing (IVC) and exhaust valve opening (EVO). In this case, the combustion chamber is considered as an open system because of the blow-by and fuel injection. The mean gas temperature in the chamber is calculated using the ideal gas equation of state. In addition, the gas thermodynamic conditions in the chamber are obtained through the in-cylinder pressure signal, and are used to feed the models used for estimating the convective and radiative heat transfer [40]. Moreover, the thermodynamic conditions are used as input for the filling-emptying model, which provides the fluid-dynamic conditions in the ports and the heat transfer flows in these elements. The wall temperatures are calculated by means of a lumped conductance model, which is connected to the heat transfer models.

The main results from CALMEC used in this investigation are the instantaneous rate of heat release (RoHR) and bulk gas temperature, and some parameters to describe the combustion process, such as the start of combustion (CA10), combustion center (CA50) and combustion duration (CA90-CA10).

2.4. Engine testing methodology

The potential of the different fuels is evaluated in four operating points, whose main engine settings are shown in Table 3. The tests proposed are representative of the conditions found in the NEDC for a vehicle of an inertia weight class of 1590 kg [42]. As

shown in Table 3, the CA50 and NOx emissions were kept constant for each operating point. To achieve this, the EGR rate and SOI were modified simultaneously for each fuel tested.

Figure 2 shows the results of the sweeps performed to reach the CA50-NOx target with the different fuels. For the sake of brevity, the figure only shows the results for the test point LP1, while a summary of the four conditions is shown in Table 4. Due to its more different properties, the sweep of 1-octanol is not shown in Figure 2, but its selected conditions are depicted in Table 4. As it can be seen from Figure 2, the EGR rate needed to maintain the CA50 constant for all the fuels was very similar, with a maximum variation of 0.4% in the case of the DNBE. Thus, the CA50 was mainly controlled by the SOI, which had to be delayed as the fuel CN increased. The values that allow reaching the CA50-NO_x target for each fuel are marked in the figure with a vertical line, and the NO_x emissions for these points are also shown in lower part of the graph.

Table 3. Engine operating conditions.

Test [-]	Engine speed [1/min]	IMEP [bar]	CA50 [CAD aTDC]	Pilot offset [CAD]	DOI pilot injection [us]	Rail pressure [bar]	Boost pressure [bar]	Exhaust back pressure [bar]	Intake air temp. [ºC]	Oil temp. [ºC]	Water temp. [ºC]	EU6 [g/kWh]
LP1	1500	4.3	6.6	10	180	720	1.07	1.13	25	90	90	0.2
LP2	1500	6.8	5.8	11	140	900	1.5	1.6	30	90	90	0.2
LP3	2280	9.4	9.2	20	120	1400	2.29	2.39	35	90	90	0.4
LP4	2400	14.8	10.8	28	120	1800	2.6	2.8	45	90	90	0.6

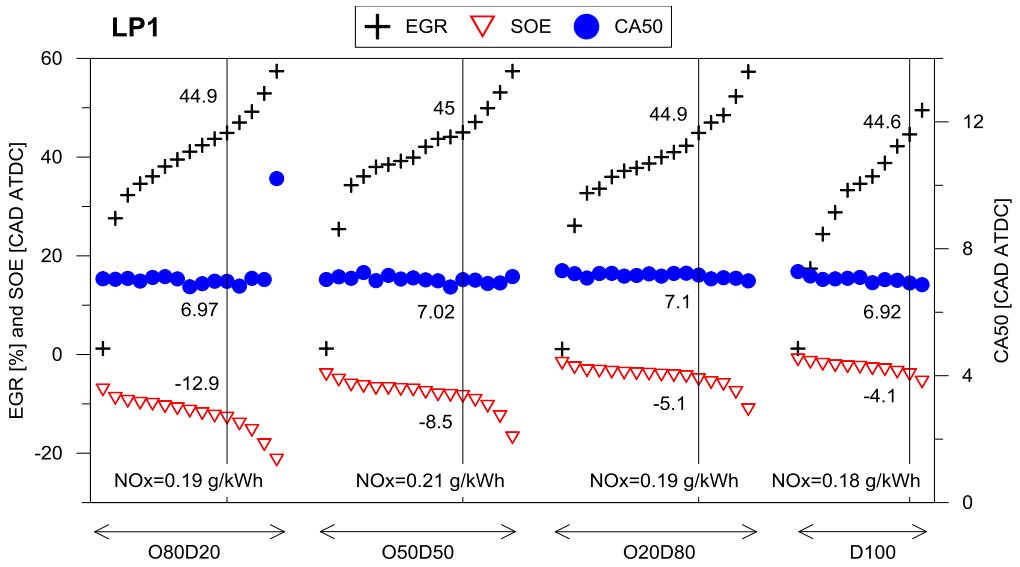

Figure 2. Engine settings needed to reach the CA50-NOx target for each fuel in the load point LP1.

Table 4. Engine parameters for each fuel and operating point.

Fuel [-]	LP1 (1500/4.3)			LP2 (1500/6.8)			LP3 (2280/9.4)			LP4 (2400/14.8)		
	CA50 [CAD aTDC]	SOI [CAD aTDC]	EGR [%]	CA50 [CAD aTDC]	SOI [CAD aTDC]	EGR [%]	CA50 [CAD aTDC]	SOI [CAD aTDC]	EGR [%]	CA50 [CAD aTDC]	SOI [CAD aTDC]	EGR [%]
1-Oct	6.6	-19.9	41.6	6.1	-13	43.5	8.8	-7.7	40.5	8.9	-6	31
O80D20	6.97	-12.9	44.9	6.22	-7.3	45.9	8.64	-4.2	42.7	8.7	-6	33.6
O50D50	7.02	-8.5	45	5.97	-5	44.7	8.2	-4.5	43.4	8.3	-6.6	34.6
O20D80	7.17	-5.1	44.9	5.71	-4.6	46.3	7.63	-5.2	43.6	8.4	-6.6	34.1
DNBE	6.92	-4.1	44.6	5.37	-4.5	45	8.25	-5.2	43.9	8.5	-7.2	34.4
Diesel	7.94	-6.4	44.1	5.75	-2.7	45.1	8.04	-1.5	43.8	8.6	-6.5	33.2

3. Results and discussion

This section compares the combustion characteristics of the different fuels as well as their emissions and performance for the operating conditions described in the subsection 2.4. Figure 3 shows the RoHR and in-cylinder temperature profiles for the different fuels in the LP1 condition. As it can be seen, all the biofuels show a Gaussian-shaped heat release with similar combustion onset (CA10). After the start of combustion (SOC), the fuel reactivity seems to play a key role on the combustion development. In this sense, the maximum RoHR peak is highest for the blends having 1-octanol percentages up to 50%, leading also to shorter combustion duration. With 1-octanol contents greater than 50%, the RoHR peak decreases and the combustion duration increases. On the other hand, the diesel fuel shows the largest combustion duration due to the slow combustion during the expansion period, which will penalize the fuel-to-work conversion efficiency (Figure 5). In terms of in-cylinder temperature, 1-octanol shows the lowest values because it has the highest heat of vaporization (HoV) and the lowest EGR rate. Since the fuel blends have similar EGR rate than diesel, the lower temperature is consequence of the lower HoV. Finally, Table 2 shows that the HoV for DNBE is lower than for diesel, but the lower heating value (LHV) is lower in a greater extent, so that the fuel mass needed to be injected is greater, and the cooling effect is more notable.

Regarding the engine-out emissions, Figure 4 shows that all the fuels are able to perform within the NO_x limit imposed of 0.2 g/kWh, with the slight differences being consequence of the variations in the engine parameters needed to fulfill the CA50-NO_x target with each fuel. Focusing on the biofuels, it is seen that HC and CO emissions increase with the 1-octanol percentage in the blend. This is related to the lower fuel reactivity, which worsens the combustion progression towards the critical zones of the combustion chamber. However, the CO levels found with the biofuels are lower than with diesel. This is expected to be consequence of the greater oxygen content in the fuel molecule, which benefits the CO to CO_2 conversion reactions. Soot emissions are negligible for all the fuels due to the premixed nature of the combustion, three of them providing values below the smoke meter measurement range.

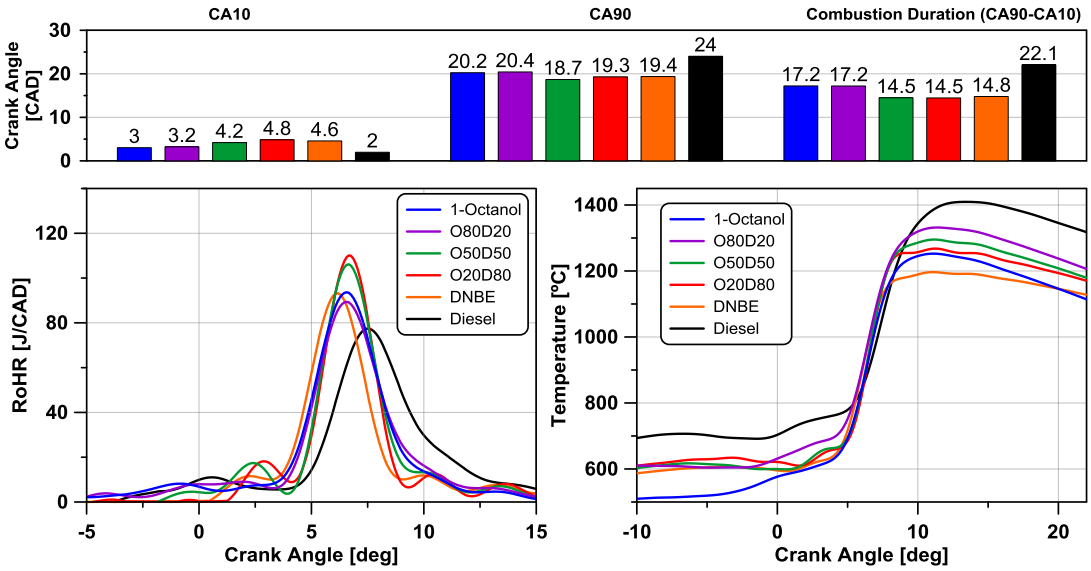

Figure 3. RoHR and in-cylinder temperature for the different fuels in the LP1 condition.

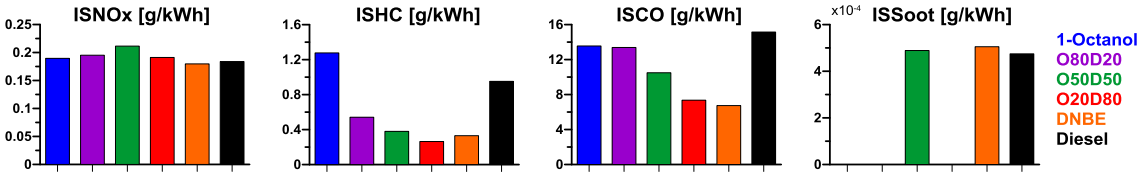

Figure 4. Engine-out emissions for the different fuels in the LP1 condition.

Figure 5 shows the fuel energy apportionment among the different outgoing energy paths for the different fuels in the LP1 condition. In Figure 5, the term *GI work* accounts for the work output from the cycle without discounting the pumping work, the term *heat transfer* accounts for the energy rejected by heat transfer to the ambient, coolant and oil, the term *exhaust losses* accounts for the net flow of sensible enthalpy in the exhaust stream, and the term *combustion losses* accounts for the energy loss because not all the injected fuel is burned during the combustion cycle. As it can be seen, all the biofuels provide higher gross indicated efficiency (GIE) than diesel fuel, with a net efficiency improvement that ranges from 0.9 to 2.8%. Part of the efficiency increase comes from the combustion losses reduction. As it can be seen, all the biofuels except the 1-octanol allow reducing the combustion losses versus diesel. Moreover, it is seen that the benefit versus diesel reduces as the 1-octanol percentage in the blend increases. This is expected to be consequence of the lower reactivity of the in-cylinder mixture due to the addition of 1-octanol, which leads to greater amount of unburned fuel during combustion. Nevertheless, the key point to explain the efficiency increase with the biofuels is the notable heat transfer (HT) reduction. As it can be seen, the use of 1-octanol allows reducing the energy rejected by heat transfer to the coolant fluids and ambient by 5.8% versus diesel due to the low in-cylinder temperature during the cycle. However, the exhaust losses for 1-octanol are 2.9% higher than with diesel, which penalizes the net efficiency improvement. The difference in the exhaust losses is related to differences in the exhaust mass flow due to using different EGR rates (41.6% vs 44.1%). In any case, from the efficiency

standpoint, the relationship between these two energy paths is more beneficial for the 1-octanol than the rest of biofuels, which show similar performance.

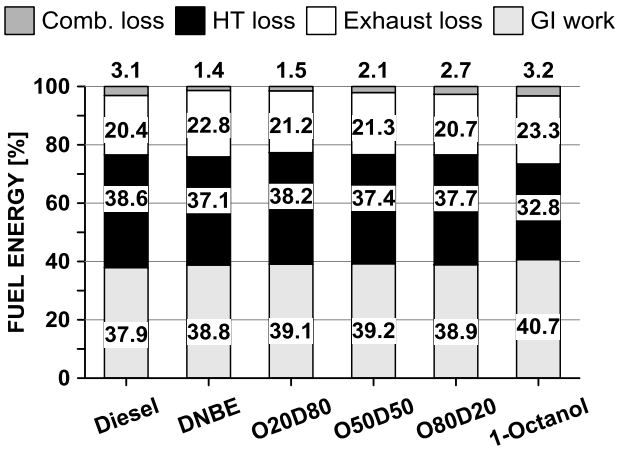

Figure 5. Fuel energy apportionment among the different outgoing energy paths for the different fuels in the LP1 condition.

Figure 6 shows the RoHR and temperature profiles for the different fuels in the LP2 condition. Focusing on the behavior of the different blends, it is clear that the RoHR peak increases as the fuel CN decreases. This occurs due to the extended mixing time achieved with low CN, which leads to more premixed combustion. By contrast, the high CN of DNBE results in the earliest autoignition, leading to a more sequential heat release. Regarding the engine-out emissions shown in Figure 7, it is seen that all the blends allow reaching the NOx target, which is 0.2 g/kWh for this condition. The NOx differences between the blends are related to differences in the individual calibration. The use of 1-octanol leads to the greatest NOx level due to the high RoHR peak, which in turn leads to high in-cylinder pressure and temperature peaks. On the other hand, the EGR effect on emissions can be observed by comparing the data corresponding to O50D50 and O80D20. As it can be seen, the RoHR peak with O50D50 is lower than O80D20, but the EGR rate used is also lower (44.7% vs 45.9%), which makes the O50D50 to produce more NOx during combustion. Soot emissions are proportional to the DNBE content in the blends. Since DNBE and 1-octanol have the same oxygen content, the soot reduction is expected to be consequence of the extended mixing time achieved as the 1-octanol percentage increases, which leads to leaner equivalence ratios regions at SOC. The diesel fuel promotes higher soot content than the rest of fuels due to its reduced oxygen content and aromatic compounds. No soot emission could be detected for 1-octanol due to using the lowest EGR rate of the investigated fuels and the greatest mixing time before combustion. Finally, the figure shows that HC and CO emissions increase with the 1-octanol content. This is expected to occur due to the lower in-cylinder mixture reactivity, which leads to flame quenching at the critical zones of the combustion chamber, as in the crevices and near the cylinder-liner regions. CO emissions with diesel fuel are expected to be high due to the more diffusive characteristic (lower mixing time) and the lower oxygen content in the fuel molecule.

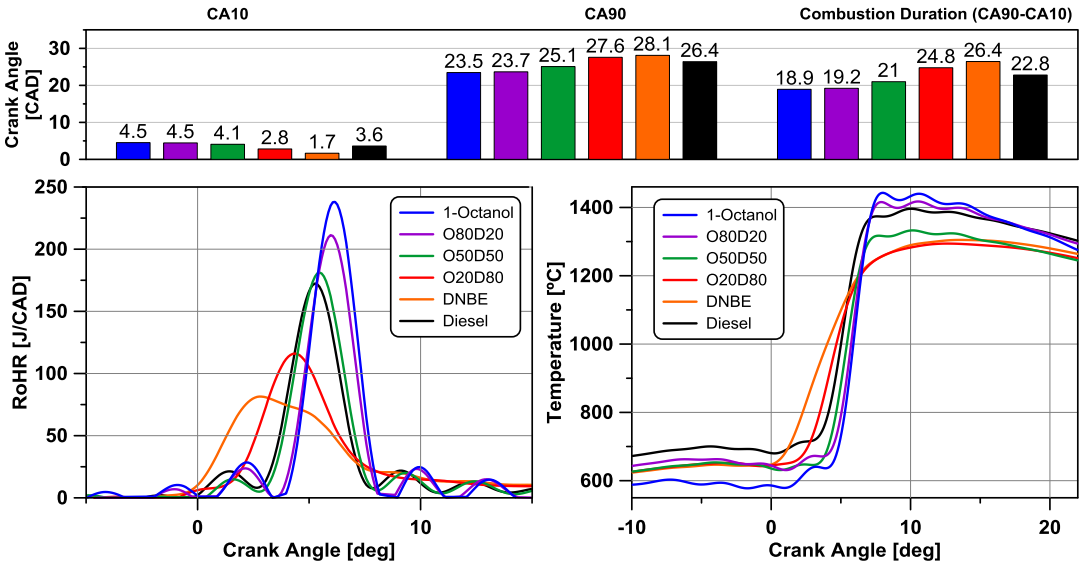

Figure 6. RoHR and in-cylinder temperature for the different fuels in the LP2 condition.

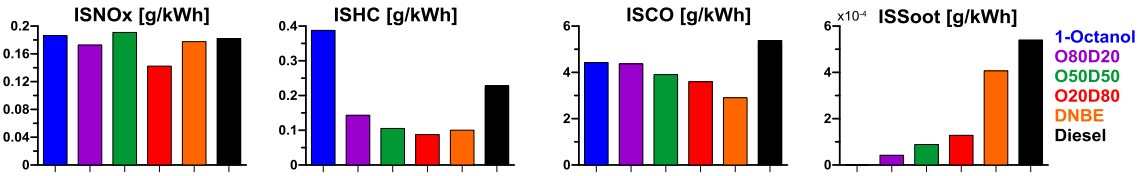

Figure 7. Engine-out emissions for the different fuels in the LP2 condition.

In terms of engine efficiency, Figure 8 shows the fuel energy apportionment for the different tests in the LP2 condition. As it can be seen, all the fuels tested allow increasing the GIE versus diesel, with the net improvement ranging from 0.7 to 1.8%. As it can be seen, the main driver for the GIE increase is the HT reduction. Nonetheless, the exhaust losses also increase to some extent, so that the net benefit in GIE because of the HT reduction is penalized. In any case, exhaust losses are preferable than HT because the thermal enthalpy of the exhaust stream is beneficial for increasing the efficiency of the aftertreatment systems. As Figure 8 shows, the fuel enabling the greatest fuel-to-work conversion is the 1-octanol. In spite of having equal combustion losses than diesel, the HT losses are reduced in a higher extent than the exhaust losses increase. The HT reduction is explained comparing the in-cylinder temperature and combustion duration values shown in Figure 6. As it can be seen, the in-cylinder temperature with 1-octanol is lower than with diesel during almost all the cycle, with the exception of the range from +7 to +17 CAD ATDC, in which both temperatures are very similar. Thus, the lower combustion duration with 1-octanol allows reducing the energy rejected to the coolant by HT (18.9 CAD vs 22.8 CAD). It is interesting to note that all the fuels lead to lower in-cylinder temperatures than diesel before the start of combustion. In the case of the fuels containing 1-octanol, this is consequence of the higher HoV. In the case of DNBE, this is consequence of the slightly lower LHV than diesel, which entails injecting greater fuel mass per cycle overcompensating the lower HoV.

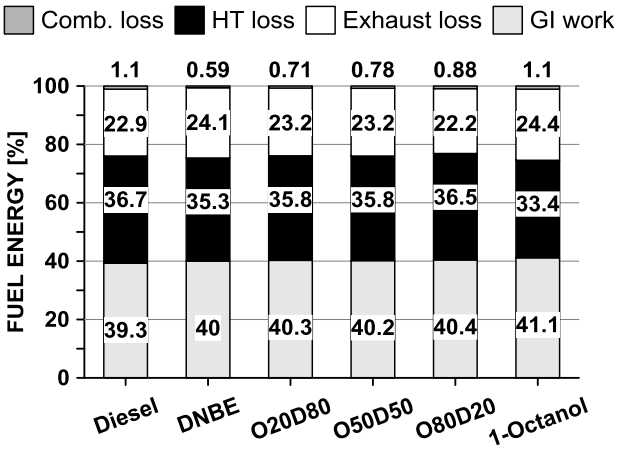

Figure 8. Fuel energy apportionment among the different outgoing energy paths for the different fuels in the LP2 condition.

Figure 9 shows the RoHR and temperature profiles for the different fuels in the LP3 condition. As it can be seen, the start of combustion is dominated by the fuel blend composition. In this sense, 1-octanol shows the most delayed SOC, while DNBE has the earliest combustion onset due to its high CN. Again, it is confirmed that the RoHR for the diesel fuel evolves very similar to O50D50, as was shown in Figures 3 and 6. However, the rest of fuels show different RoHR evolution than the others. In this sense, the high premixing degree achieved with 1-octanol leads to a Gaussian-shaped RoHR. As the 1-octanol content in the mixture reduces, the mixing time diminishes, evidencing more the second RoHR peak corresponding to the diffusive combustion period. The diesel fuel shows a transitional behavior with two RoHR peaks of similar magnitude. Finally, O20D80 and DNBE show a moderate premixed phase with more diffusive combustion due to the high CN of these fuels.

Figure 10 shows the engine-out emissions for the LP3 engine load point. All the tests have similar levels of NOx emissions, near the limit of 0.4 g/kWh. The HC emissions trend with the fuel blend composition is inverse to that found in LP1 and LP2 conditions. In this case, the addition of 1-octanol up to 80% reduces the HC emissions. This result agrees with previous findings found in literature, which reports lower HC emissions for 1-octanol as engine load increases because the high gas temperatures are sufficient for post-oxidization of unburned HC [31]. The CO emissions increase as the percentage of 1-octanol in the blend increases. This can be explained looking at the in-cylinder temperature profiles. As it can be seen, the maximum temperature decreases with the addition of 1-octanol, which worsens the CO to CO_2 conversion reactions. In the case of 1-octanol, the maximum temperature is in the limit of activating the conversion reactions, leading to the highest amount of CO emissions. Finally, it is seen that soot emissions are negligible for all the fuels, being the soot levels emitted with diesel around ten times greater than the other fuels. The high soot levels with diesel are explained by the high EGR rate used (Table 4) together with the low oxygen content of the fuel and aromatic compounds.

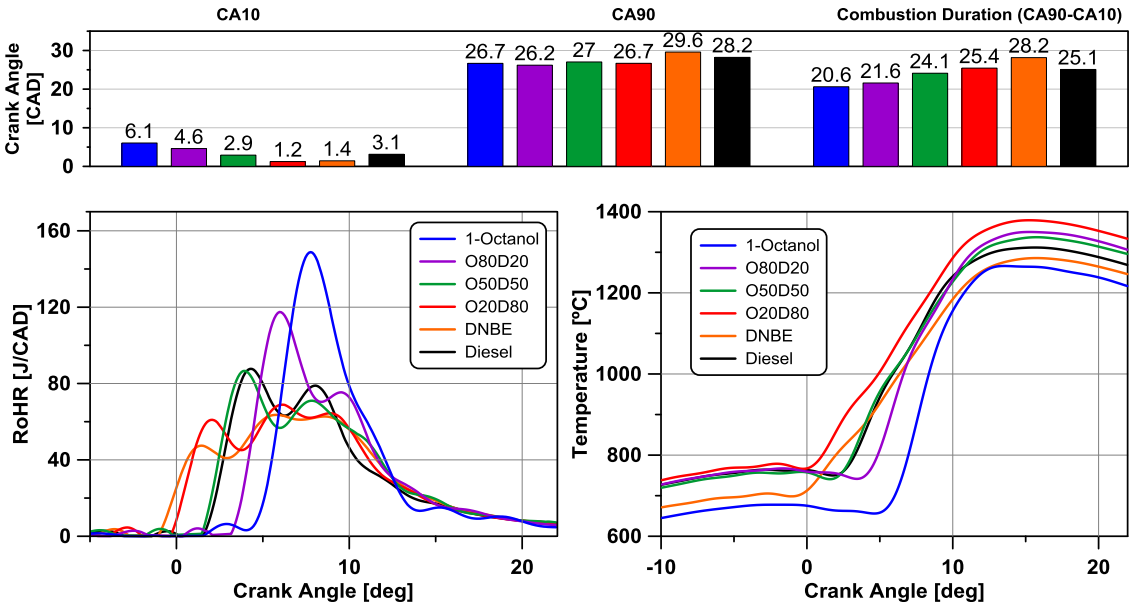

Figure 9. RoHR and in-cylinder temperature for the different fuels in the LP3 condition.

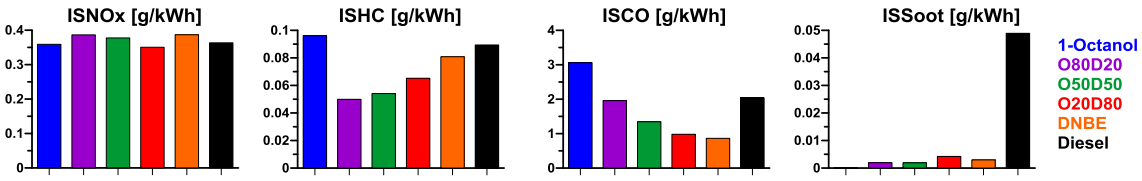

Figure 10. Engine-out emissions for the different fuels in the LP3 condition.

Figure 11 shows the fuel energy distribution for the different fuels in the LP3 condition. As it can be seen, all the fuels allow increasing the GIE versus diesel fuel. In this case, there is not a general trend on the energy pathway between the different fuels. It is clear that combustion losses increase with the 1-octanol content in the blend, with all the fuels except the 1-octanol showing lower combustion losses than with diesel. Regarding the three intermediate blends (O20D80, O50D50 and O80D20), they show greater HT losses than diesel and the pure fuels. This is because of the higher in-cylinder temperature (Figure 9). However, the higher temperature during the expansion stroke results in higher exhaust losses. Finally, the main benefit in GIE with DNBE and 1-octanol comes from a reduction in HT due to the lower in-cylinder temperature, while the exhaust losses increase. Globally, the fuel that offers the highest efficiency is O20D80. However, 1-octanol could be also interesting because it only has 0.2% lower GIE than O2080, but changes a lot the apportionment between HT and exhaust losses, which is an important factor from the aftertreatment systems standpoint.

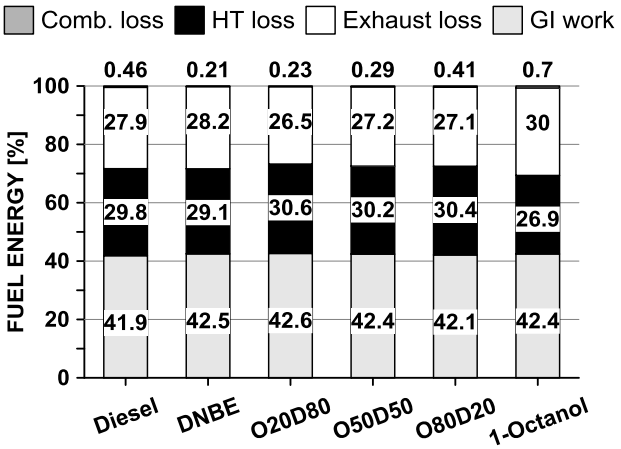

Figure 11. Fuel energy apportionment among the different outgoing energy paths for the different fuels in the LP3 condition.

Figure 12 shows the RoHR profiles and the engine-out emissions for the different fuels in the LP4 condition. As it can be seen, all the RoHR profiles have a diesel-like shape with a premixed combustion phase first, followed by a diffusion period and a diesel-like tail during the late combustion. The start of combustion is clearly correlated with the blend composition. As the percentage of 1-octanol in the blend increases, the start of combustion is more delayed. This occurs due to the lower reactivity (i.e., CN) of the blend. The extended mixing time allows more fuel amount to be premixed, leading to higher RoHR peak in this combustion phase. Since the end of the diffusive period is similar to all the fuels with the exception of diesel, the combustion duration shows a decreasing trend with the 1-octanol percentage. The diesel fuel shows faster reactions at the end of combustion, which should be consequence of the higher in-cylinder temperatures. As shown in Figure 13, all the fuel blends provide NOx levels below 0.6 g/kWh, which was the limit imposed for this operating point. Due to the high heat of vaporization of 1-octanol, its in-cylinder temperature is the lowest in spite of the premixed RoHR peak, which allows controlling the NOx emissions. The soot emissions show ultra-low levels for all the blends with the exception of O50D50. This is not explained looking at the RoHR profiles, since that of O50D50 shows an intermediate behavior compared to the other fuels. Thus, the main cause for the highest soot levels with O50D50 seems to be the highest EGR rate (34.6%), which in turn leads to the lowest NOx emissions. A measurement error can also be the cause considering that the soot level for O50D50 is 5 times greater than for the rest of the blends. Furthermore, the soot emissions at even lower NOx emissions (0.55 g/kWh) are in the order of magnitude of the other blends. Finally, the HC emissions show the same behavior than that found in the LP3 condition, with the highest level found for the 1-octanol due to its low CN and in-cylinder temperature. The CO levels are below 0.8 g/kWh in all the cases, with the exception of the diesel fuel, as found in LP1 and LP2 operating conditions.

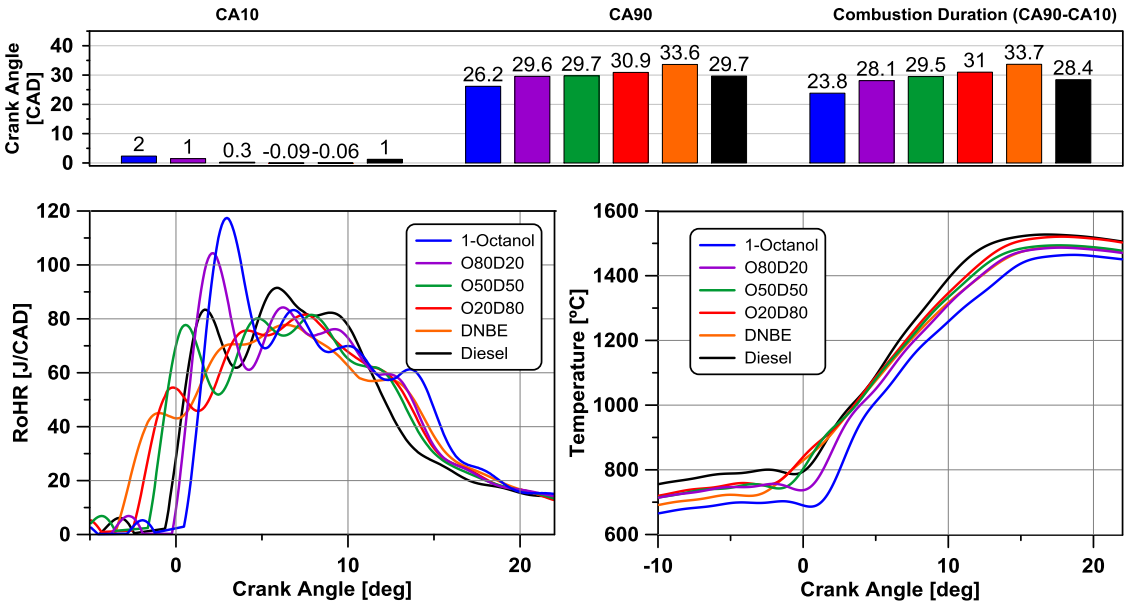

Figure 12. RoHR and in-cylinder temperature for the different fuels in the LP4 condition.

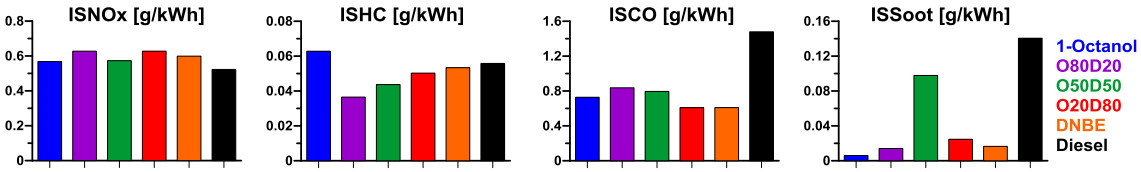

Figure 13. Engine-out emissions for the different fuels in the LP4 condition.

Figure 14 shows the fuel energy apportionment among the different outgoing paths for the different fuels in the LP4 condition. As it can be seen, all the fuels tested provide equal or higher GIE than the reference diesel. The 1-octanol leads to the same GIE than diesel, but with a substantially different energy apportionment. In this sense, the 1-octanol reduces the HT losses by 2.55%. However, this energy is not converted in indicated work because of the increased exhaust losses (+2.67%). The exhaust losses increase is driven by the higher heat release during the late combustion period (≈+15 CAD ATDC). The incomplete combustion with 1-octanol is reduced to halve versus diesel, which is also observed for the rest of the fuels. Finally, the O20D80 blend leads to the highest GIE (+1% compared to diesel) thanks to the simultaneous reduction of all the losses.

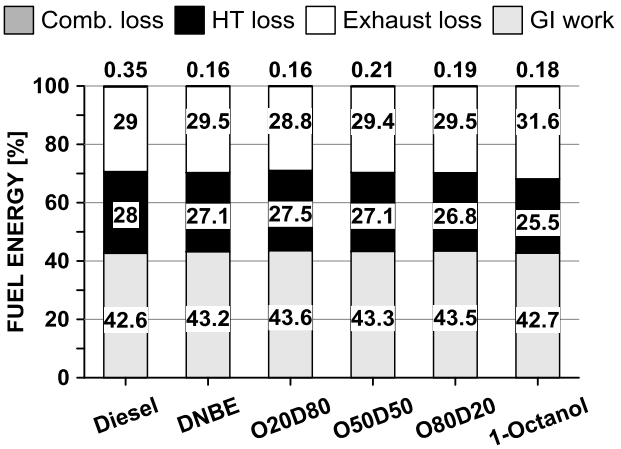

Figure 14. Fuel energy apportionment among the different outgoing energy paths for the different fuels in the LP4 condition.

4. Conclusions

This paper evaluated the performance of several tailor-made fuels from biomass as potential candidates to be used in compression ignition engines. Two base fuels, 1-octanol and DNBE, together with three intermediate blends of these two fuels (20%-80%, 50%-50% and 80%-20%) were tested in a single-cylinder light-duty engine. The engine operating conditions selected to evaluate the potential of the fuels were 1500 rpm/4.3 bar, 1500 rpm/6.8 bar, 2280 rpm/9.4 bar and 2400 rpm/14.8 bar. The combustion process, performance and engine-out emissions with these fuels were analyzed and compared to diesel fuel. The more relevant results can be summarized as follows:

- The instantaneous RoHR with the reference diesel fuel is very similar to the blend O50D50 in all the operating conditions, due to a very similar cetane number.
- The differences in CN between the different fuels result in different combustion behavior at 2280 rpm/9.4 bar. The fuel blends with low CN lead to a Gaussian-shaped RoHR, while high CN fuels lead to a diffusive-shape RoHR.
- The higher oxygen content of the biomass-derived fuels promote a notable reduction of soot emissions versus diesel fuel for the same NOx levels.
- The biomass-derived fuels have the same oxygen content. Thus, the difference in soot emissions between them are related to different in mixing time due to differences in CN.
- The alternative fuels improve the fuel-to-work conversion efficiency versus diesel due to a better balance among heat transfer and exhaust losses. Moreover, all the fuels with the exception of 1-octanol are able to promote a substantial reduction of the combustion losses versus the diesel fuel.
- The use of 1-octanol leads to the highest gross indicated efficiency at 4.3 and 6.8 bar. As load increases, at 9.4 and 14.8 bar, the most efficient fuel is O20D80 thanks to its great reduction in exhaust losses.

Generally, it can be stated that for the investigated fuels, lower reactivity is more beneficial for an increased efficiency at lower loads due to the more premixed character of the combustion. Therefore, the heat transfer losses decrease greater than

the exhaust losses and incomplete combustion increases. Additionally, the shift from heat transfer losses to the exhaust is beneficial for the aftertreatment management, which has great importance at low loads.

At high loads the higher reactivity leads to low amounts of unburnt fuel, but increased HT losses due the longer combustion duration and higher in-cylinder temperatures. However, the exhaust losses decrease results in higher gross indicated efficiencies.

Acknowledgments

The authors gratefully acknowledge FEDER and Spanish Ministerio de Economía y Competitividad for partially supporting this research through TRANCO project (TRA2017-87694-R). This work was performed as part of the Cluster of Excellence ‘‘Tailor-Made Fuels from Biomass,’’ which is funded by the Excellence Initiative by the German federal and state governments to promote science and research at German universities. Thus, the authors would like to thank the Institute for Combustion Engines, RWTH Aachen University, for all the support to perform the research activities.

References

[1] Araghi Y, Kroesen M, Van Wee B. Identifying reasons for historic car ownership and use and policy implications: An explorative latent class analysis. Transport Policy, Volume 56, May 2017, Pages 12-18.

[2] González J, Otsuka Y, Araki M, Shiga S. Impact of new vehicle market composition on the light-duty vehicle fleet CO2 emissions and cost. Energy Procedia, Volume 105, May 2017, Pages 3862-3867.

[3] Sun K, Chen X, Wang J, Zhang T, Zhu Z. Investigation of air quality over the largest city in central China using high resolution satellite derived aerosol optical depth data. Atmospheric Pollution Research, Volume 9, Issue 3, May 2018, Pages 584-593.

[4] Li W, Cocker D. Secondary organic aerosol and ozone formation from photo-oxidation of unburned diesel fuel in a surrogate atmospheric environment. Atmospheric Environment, Volume 184, July 2018, Pages 17-23.

[5] Singh S, Kennedy C. Estimating future energy use and CO2 emissions of the world's cities. Environmental Pollution, Volume 203, August 2015, Pages 271-278.

[6] García-Valladolid P, Tunestal P, Monsalve-Serrano J, García A, Hyvönen J. Impact of diesel pilot distribution on the ignition process of a dual fuel medium speed marine engine. Energy Conversion and Management, Volume 149, 1 Oct 2017, Pages 192-205.

[7] Benajes J, García A, Monsalve-Serrano J, Boronat V. Gaseous emissions and particle size distribution of dual-mode dual-fuel diesel-gasoline concept from low to full load. Applied Thermal Engineering, Volume 120, 25 Jun 2017, Pages 138-149.

[8] Benajes J, García A, Monsalve-Serrano J, Balloul I, Pradel G. Evaluating the reactivity controlled compression ignition operating range limits in a high-compression ratio medium-duty diesel engine fueled with biodiesel and ethanol. International Journal of Engine Research, Volume 18 (1-2), Pages 66-80, 2017

[9] Kwon Noh I, No S-Y. Effect of bioethanol on combustion and emissions in advanced CI engines: HCCI, PPC and GCI mode – A review. Applied Energy, Volume 208, 15 December 2017, Pages 782-802.
[10] Jansen A, Kremer F, Baron J, Muether M, et al. Tailor-Made Fuels from Biomass for Homogeneous Low-Temperature Diesel Combustion. Energy Fuels 25(10):4734-4744, 2011, doi:10.1021/ef2010139.
[11] Heuser B, Mauermann P, Wankhade R, Kremer F, et al. Combustion and emission behavior of linear C8 –oxygenates. International Journal of Engine Research 16/(5):627-638, 2015, doi:10.1177/1468087415594951.
[12] Marquardt W, Harwardt A, Hechinger M, Kraemer K, et al. The biorenewables opportuninty - toward next regeneration process and product systems. AIChE J.;n/a-n/a, 2010, doi:10.1002/aic.12380.
[13] Jager G, Buchs, J. Biocatalytic conversion of lignocellulose to platform chemicals. Biotechnology journal 7(9): 1122-1136, 2012, doi: 10.1002/biot.201200033.
[14] Hechinger M. Model-based Identification of Promising Biofuel Candidates for Spark-ignited Engines. Dissertation, Process Systems Engineering, Aachen, 2014.
[15] Dahmen M, Hechinger M, Victoria Villeda J, Marquardt W. Towards Model-Based Identification of Biofuels for Compression Ignition Engines. SAE Int. J. Fuels Lubr. 5(3):990-1003, 2012, doi:10.4271/2012-01-1593.
[16] Hoppe F, Heuser B, Thewes M, Kremer F, et al. Tailor-made fuels for future engine concepts. International Journal of Engine Research 17(1):16-27, 2016, doi:10.1177/1468087415603005.
[17] Julis J, Hölscher M, Leitner W. Selective hydrogenation of biomass derived substrates using ionic liquid-stabilized ruthenium nanoparticles. Green Chem. 12(9):1634, 2010, doi:10.1039/c004751a.
[18] Julis J, Leitner W. Synthesis of 1-octanol and 1,1-dioctyl ether from biomass-derived platform chemicals. Angewandte Chemie (International ed. In English) 51(34):8615-8619, 2012, doi:10.1002/anie.201203669.
[19] Luska K, Julis J, Stavitski E, Zakharov D, et al. Bifunctional nanoparticle-SILP catalysts (NPs@SILP) for the selective deoxygenation of biomass substrates. Chem. Sci. 5(12):4895-4905, 2014, doi:10.1039/C4SC02033B.
[20] Kumar B, Saravanan S, Rana D, Nagendran A. A comparative analysis on combustion and emissions of some next generation higher-alcohol/diesel blends in a direct-injection diesel engine. Energy Conversion and Management, Volume 119, 1 July 2016, Pages 246-256.
[21] Raffius T, Ottenwälder T, Schulz C, Grünefeld G, Koß H, Pischinger S. Laser spectroscopic investigation of diesel-like jet structure using C8 oxygenates as the fuel. Fuel, Volume 235, 1 January 2019, Pages 1515-1529.
[22] Kalim Akhtar M, Dandapani H, Thiel K, Jones P. Microbial production of 1-octanol: A naturally excreted biofuel with diesel-like properties. Metabolic Engineering Communications, Volume 2, December 2015, Pages 1-5.
[23] Kumar B, Saravanan S, Rana D, Anish V, Nagendran A. Effect of a sustainable biofuel – n-octanol – on the combustion, performance and emissions of a DI diesel engine under naturally aspirated and exhaust gas recirculation (EGR) modes. Energy Conversion and Management, 118 (2016), pp. 275-286.

[24] Cai L, Uygun Y, Togbé C, Pitsch H, Olivier H, Dagaut P, Mani Sarathy S. An experimental and modeling study of n-octanol combustion. Proceedings of the Combustion Institute, Volume 35, Issue 1, 2015, Pages 419-427.
[25] Gopal K, Sathiyagnanam A, Kumar B, Saravanan S, Rana D, Sethuramasamyraja B. Prediction of emissions and performance of a diesel engine fueled with n-octanol/diesel blends using response surface methodology. Journal of Cleaner Production, Volume 184, 20 May 2018, Pages 423-439.
[26] Ashok B, Nanthagopal K, Anand V, Aravind K, Jeevanantham A, Balusamy S. Effects of n-octanol as a fuel blend with biodiesel on diesel engine characteristics. Fuel, Volume 235, 1 January 2019, Pages 363-373.
[27] Kerschgens B, Caia L, Pitsch H, Heuser B, Pischinger S. Di-n-buthylether, n-octanol, and n-octane as fuel candidates for diesel engine combustion. Combustion and Flame, Volume 163, January 2016, Pages 66-78.
[28] Geilen F, Engendahl B, Harwardt A, Marquardt W, et al. Selective and Flexible Transformation of Biomass-Derived Platform Chemicals by a Multifunctional Catalytic System. Angewandte Chemie 122(32):5642-5646, 2010, doi:10.1002/ange.1201002060.
[29] Ottenwaelder T, Pischinger S. Effects of Biofuels on the Mixture Formation and Ignition Process in Diesel-Like Jets. SAE Technical Paper 2017-01-2332, 2017, doi:10.4271/2017-01-2332.
[30] Mühlbauer W, Lorenz S, Brueggemann D. Optical Studies on the Influence of di-n-butyl ether (DNBE) on Combustion and Partical Number Emissions. doi:10.4271/2015-24-2482.
[31] Heuser B, Laible T, Jakob M, Kremer F, et al. C8-Oxygenates for Clean Diesel Combustion. SAE Technical Paper 2014-01-1253, 2014, doi:10.4271/2014-01-1253.
[32] Zubel M, Pischinger S, Heuser B. Assessment of the Full Thermodynamic Potential of C8-Oxygenates for Clean Diesel Combustion. SAE Int. J. Fuels Lubr. 10(3):2017, https://doi.org/10.4271/2017-24-0118.
[33] Muether M, Lamping M, Kolbeck A, Cracknell R. Advanced Combustion for Low Emissions and High Efficiency Part 1: Impact of Engine Hardware on HCCI Combustion, SAE Techinical Paper 2008-01-2405. http://dx.doi.org/10.4271/2008-01-2405.
[34] Martín J, Novella R, García A, Carreño R, Heuser B, Kremer F, Pischinger S. Thermal analysis of a light-duty CI engine operating with diesel-gasoline dual-fuel combustion mode. Energy, Volume 115, Part 1, 15 November 2016, Pages 1305-1319.
[35] TOXNET Toxicity data network. http://toxnet.nlm.nih.gov/.
[36] Pubchem open chemistry database. https://pubchem.ncbi.nlm-nih.gov/.
[37] Yaws C. Thermophysical properties of chemicals and hydrocarbons. William Andre, Norwich, N.Y., ISBN 978-0-8155-1596-8, 2008.
[38] Yaws C. Transport properties of chemical and hydrocarbons: Viscosity, thermal conductivity, and diffusivity of C1 to C100 organics and Ac to Zr inorganics / Carl L. Yaws. William Andrew, Norwich, N.Y., ISBN 978-0-8155-2039-9, 2009.
[39] Seidenspinner P, Härtl M, Wilharm T, Wachtmeister G. Cetane Number Determination by Advanced Fuel Ignition Delay Analysis in a New Constant Volume Combustion Chamber. SAE Technical Paper 2015-01-0798, 2015, doi:10.4271/2015-01-0798.

[40] Payri F, Olmeda P, Martin J, Carreño R. A New Tool to Perform Global Energy Balances in DI Diesel Engines, SAE Int. J. Engines. http://dx.doi.org/10.4271/2014-01-0665.
[41] Benajes J, Olmeda P, Martín J, Carreño R. A new methodology for uncertainties characterization in combustion diagnosis and thermodynamic modelling. Applied Thermal Engineering, 71 (2014), pp. 389-399.
[42] Heuser B, Jakob M, Kremer F, Pischinger S, Kerschgens B, Pitschet H. Tailor-Made Fuels from Biomass: Influence of Molecular Structures on the Exhaust Gas Emissions of Compression Ignition Engines. SAE Technical Paper 2013-36-0571, 2013, doi:10.4271/2013-36-0571.

Abbreviations

AFIDA: Advanced Fuel Ignition Delay Analyzer

ATDC: After Top Dead Center

CAD: Crank Angle Degree

CA10: Crank Angle corresponding to 10% of the total energy delivered

CA50: Crank Angle corresponding to 50% of the total energy delivered

CA90: Crank Angle corresponding to 90% of the total energy delivered

CI: Compression Ignition

CN: Cetane Number

CO: Carbon Monoxide

DNBE: Di-n-Butyl Ether

EGR: Exhaust Gas Recirculation

EVO: Exhaust Valve Opening

FSN: Filter Smoke Number

GIE: Gross Indicated Efficiency

HC: Hydro Carbons

HoV: Heat of Vaporization

HT: Heat Transfer

HVO: Hydrotreated Vegetable Oil

ICE: Internal Combustion Engine

IMEP: Indicated Mean Effective Pressure

IVC: Intake Valve Closing

LTHR: Low Temperature Heat Release

NEDC: New European Driving Cycle

NOx: Nitrogen Oxides

ON: Octane Number

PM: Particulate Matter

RoHR: Rate of Heat Release

SCE: Single Cylinder Engine

SOC: Start of Combustion

SOI: Start of Injection